



DRaGon: Mining Latent Radio Channel Information from Geographical Data Leveraging Deep Learning

Benjamin Sliwa¹, Melina Geis¹, Caner Bektas¹, Melisa Lopéz², Preben Mogensen², and Christian Wietfeld¹

¹Communication Networks Institute, TU Dortmund University, 44227 Dortmund, Germany

²Wireless Communication Networks, Aalborg University, 9220 Aalborg, Denmark

e-mail: ¹{firstname.lastname}@tu-dortmund.de ²{mll, pm}@es.aau.dk

Abstract—Radio channel modeling is one of the most fundamental aspects in the process of designing, optimizing, and simulating wireless communication networks. In this field, long-established approaches such as analytical channel models and ray tracing techniques represent the de-facto standard methodologies. However, as demonstrated by recent results, there remains an untapped potential to innovate this research field by enriching model-based approaches with machine learning techniques. In this paper, we present Deep Radio channel modeling from GeOinformationN (DRaGon) as a novel machine learning-enabled method for automatic generation of Radio Environmental Maps (REMs) from geographical data. For achieving accurate path loss prediction results, DRaGon combines determining features extracted from a three-dimensional model of the radio propagation environment with raw images of the receiver area within a deep learning model. In a comprehensive performance evaluation and validation campaign, we compare the accuracy of the proposed approach with real world measurements, ray tracing analyses, and well-known channel models. It is found that the combination of expert knowledge from the communications domain and the data analysis capabilities of deep learning allows to achieve a significantly higher prediction accuracy than the reference methods.

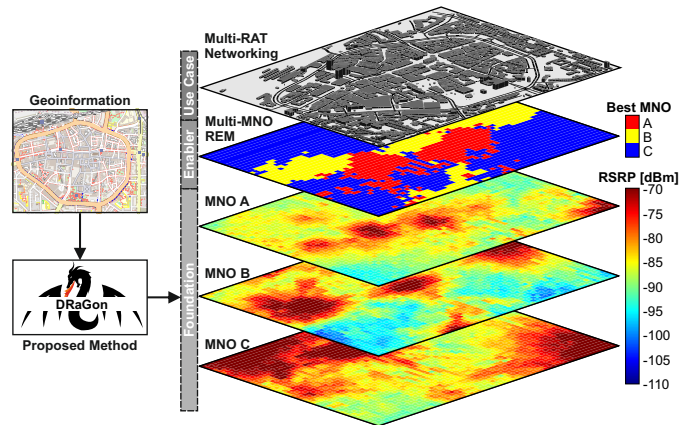


Fig. 1. Example application of the proposed DRaGon method for generating RSRP REMs for three different MNO. The acquired radio channel knowledge is aggregated in a multi-MNO map that provides the required information for performing dynamic MNO selection at the application layer (Map data: © OpenStreetMap Contributors, CC BY-SA).

I. INTRODUCTION

The ability to determine the received signal strength for a given sender and receiver pair is one of the most fundamental aspects for planning [1] and simulating [2] wireless networks. Moreover, emerging mobile communication paradigms such as anticipatory networking [3], [4] explicitly build upon using a priori context knowledge for proactive network optimization.

However, the existing model-based approaches for path loss determination heavily rely on *abstractions* and simplifications of the radio propagation environment, which limits their significance for *concrete* real world scenarios. Ray tracing [5] aims to overcome these limitations through explicit modeling of the radio propagation environment. However, in many practical scenarios, the required high resolution data about shapes and materials of the obstacles might not be available, inherently implying a significant degradation of the achievable modeling accuracy [6]. Fueled by the availability of computation power, data sets, and algorithms, machine learning has started to become an integral part of all areas related to wireless networking [7]. Due to its inherent strength of learning closed system descriptions of complex processes from measurable features, it has also become a promising method for solving

classical communication problems such as network simulation [8] and radio channel modeling [9].

In this paper, we present the novel DRaGon method for extracting latent radio channel information from widely available geographical data that builds upon the well-known strengths of deep learning-based [10] image analysis. Following the assumption that similar “looking” environments will show similar radio propagation characteristics, DRaGon not only relies on explicitly extracted features (e.g., the number of building penetrations on the direct path between sender and receiver) but also incorporates top and side view images of the receiver environment within the prediction process. Fig. 1 shows an example for the utilization of the proposed method in the context of multi-Radio Access Technology (RAT) networking. Hereby, DRaGon automatically transforms the geoinformation input data into MNO-specific REMs of the Reference Signal Received Power (RSRP). This information provides the foundation for a multi-MNO REM that allows to dynamically determine the serving MNO based on the current user position.

The remainder of the paper is structured as follows. After discussing the related work in Sec. II, we present the novel DRaGon method in Sec. III. Afterwards, an overview of the methodological aspects is given in Sec. IV. Finally, detailed

results of the achievable modeling accuracy and the generalizability of the proposed method are provided in Sec. V.

II. RELATED WORK

Anticipatory mobile networking [3] is novel paradigm in wireless communications that focuses on the exploitation of *context* information for proactive network optimization. According to a recent white paper [11] of the 5G Automotive Association (5GAA), this form of predictive Quality of Service (QoS) optimization will be one of the key enablers for future connected and autonomous driving. However, while the vehicles are able to measure the network quality at their *current* locations, they are not able to determine the corresponding information at the *future* locations along their trajectories in advance. A promising data-driven solution approach for closing these gaps is the utilization of REMs [12], [13] that map geospatial locations to corresponding previously acquired network context measurements.

Radio channel modeling — in addition to purely data-driven approaches such as mobile crowdsensing — is an important method for constructing the required REMs. An overview of the different classes of channel and propagation models for vehicular communications is given by Viriyasitavat et al. in [14]. In addition to simple analytical models — that do not integrate explicit environment modeling — such as Friis and Two-ray ground reflection, different methods have been proposed to increase the significance of the results for *concrete* evaluation scenarios. *Empirical* models, such as the 3rd Generation Partnership Project (3GPP) Urban Macro (UMa) [15] model, rely on real world measurement data for specific radio propagation *prototypes* (e.g., urban, suburban, and rural) and distinguish between Line-of-Sight (LOS) and Non-line-of-Sight (NLOS) channel characteristics based on a distance-dependent probability function. *Deterministic* channel models [16] utilize environmental models for computing the building penetrations in order to derive the total path loss by superpositioning the effects of the obstructed path and the non-obstructed path. Ultimately, computationally expensive *ray tracing* techniques [5] utilize high resolution environmental models for tracing the behavior of the emitted rays based on models for the physical processes such as reflection and refraction. In a comprehensive empirical analysis [2], Cavalcanti et al. analyzed 283 vehicular networking papers from top-tier conferences and journals. While only 83 of the 214 papers that made use of radio propagation models specified which model was used, the analysis revealed a clear dominance of simple analytical models such as Nakagami, Two-ray ground, Friis, and Rayleigh fading.

Machine learning has started to penetrate all areas related to wireless communications. Consequently, different research works have given a glimpse at the hidden potential of machine learning-enabled radio propagation modeling. A comprehensive summary of different disciplines, models, and applications of machine learning in wireless networking is provided by Wang et al. in [17]. In [18], Enami et al. present Regional Analysis to Infer KPIs (RAIK), a method for RSRP prediction through determining the most suitable path loss exponent of

a given channel model. For this purpose, the authors use a Light Detection And Ranging (LIDAR) environmental model from which statistical features, such as the percentage of the areas covered by buildings, is extracted. A related approach is proposed by Masood et al. in [19]. By combining evolved Node B (eNB)- and User Equipment (UE)-specific features with geographic information, the authors are able to achieve an Received Signal Strength (RSS) Root Mean Square Error (RMSE) of 6.2 dB in comparison to a ray tracing setup serving as the ground truth. The authors of [20], utilize aerial images of the environment between sender and receiver for classifying the radio channel into urban, suburban, and rural prototypes. For each of these, a specific path loss model is then used for performing predictions. Thrane et al. propose an even more consequent approach for the utilization of two-dimensional geoinformation in [21]. Hereby, raw aerial *images* of the receiver environment are utilized as input features for a deep neural network that learns an environment-dependent correction offset of a path loss model. This methodological approach represents the foundation for the novel DRaGon method.

III. MINING LATENT RADIO CHANNEL INFORMATION FROM GEOGRAPHICAL DATA WITH DRAGON

Problem statement: Our overall goal is to determine the RSRP at a specific receiver position \mathbf{p}_{RX} given the transmitter position \mathbf{p}_{TX} . According to the 3GPP standardization [22], the RSRP is calculated as

$$RSRP = P_{RX} - 10 \log_{10} (N_{PRB} \cdot N_{SC}) \quad (1)$$

whereas P_{RX} represents the received signal strength, N_{PRB} is the number of Physical Resource Blocks (PRBs), and N_{SC} is the number of subcarriers. N_{PRB} can be derived from the channel bandwidth B (e.g., 100 PRBs are available for 20 MHz cells) and N_{SC} is fixed to 12 for conventional Long Term Evolution (LTE) systems.

However, as P_{RX} is unknown, it is substituted with a generic link budget term $P_{RX} = P_{TX} - L + \Delta L$ that allows us to formulate

$$RSRP = \underbrace{P_{TX} - 10 \log_{10} (N_{PRB} \cdot N_{SC})}_{\text{Properties of the communication system}} - \underbrace{L}_{\text{Channel model}} + \underbrace{\Delta L}_{\text{ML-based correction}}. \quad (2)$$

Hereby, P_{TX} represents an Equivalent Isotropically Radiated Power (EIRP) description of the transmitter antenna that aggregates transmission power, antenna gains, and coupling losses. With L being an analytical path loss estimation — we utilize a 3GPP UMa B [15] model for this task — with respect to \mathbf{p}_{TX} and \mathbf{p}_{RX} , machine learning techniques are leveraged to learn a correction offset ΔL using geographical features. In the following paragraphs, a detailed description of the data processing pipeline is provided. A schematic illustration of the system architecture model of DRaGon is shown in Fig. 2.

A. Data Preprocessing and Augmentation

The goal of the initial preprocessing phase is to prepare the input data such that a three-dimensional model of the radio

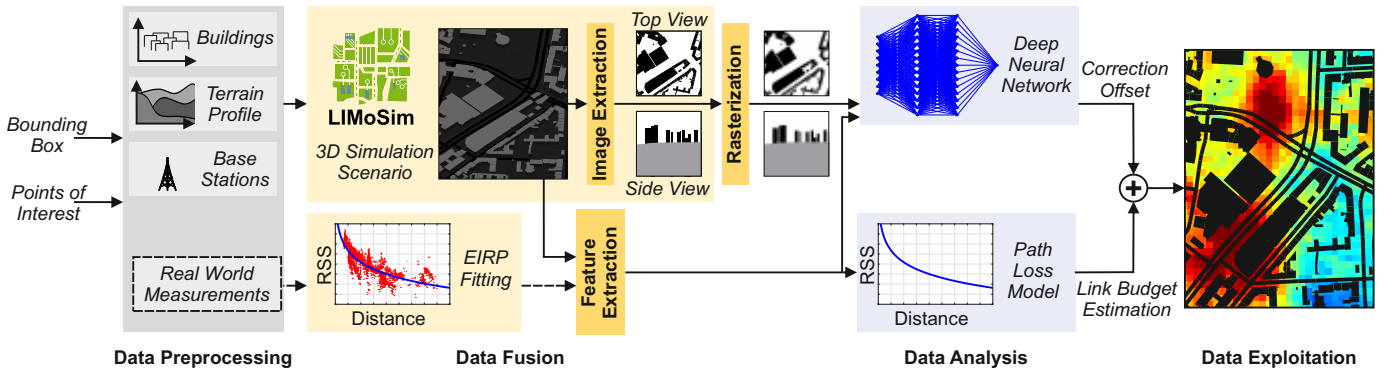


Fig. 2. Overall system architecture model of the proposed DRaGon signal strength prediction method.

propagation environment — which is capable of extracting the determining features — can be constructed.

Radio propagation environment: Publicly available OpenStreetMap (OSM) geoinformation is utilized as the main data source for building the environmental model for the given bounding box of the evaluation scenario. While the outlines of the buildings — the dominant sources of signal attenuation — are well captured within available OSM data, height information is not very well represented. As an example, from the 9630 buildings of the urban subset of the *Dortmund* scenario (see Sec. IV), only 78 are annotated with corresponding height information. In order to close these gaps, we utilize available LIDAR data for the German and Danish application scenarios. For each OSM building, the building height is calibrated with the corresponding data from the LIDAR data set whereas the matching is performed based on the respective bounding boxes.

In addition to the building-related radio propagation effects, ground reflections also have an impact on the RSRP and need to be considered. For this purpose, DRaGon incorporates data from the Digital Elevation Model over Europe (EU-DEM) [23] terrain profile that provides elevation data with 25 m cell resolution and a vertical accuracy of 7 m RMSE.

Transmission power estimation: For the application of the proposed approach, a major challenge is that information about the transmission power P_{TX} of the base stations — required for Eq. 2 — is typically not publicly available. In order to close this gap, we perform a transmission power estimation step. Hereby, we aim to find the best fit of an UMa B path loss model [15] to existing real world measurements (see Sec. IV) of the received signal strength P_{RX} . An example for the fitting process is shown in Fig. 3. For each cell, the estimated EIRP \tilde{P}_{TX} is determined by minimizing the Mean Square Error (MSE) of the N ground truth measurements and the corresponding model predictions L using the objective function

$$\min_{\tilde{P}_{TX}} \left(\frac{1}{N} \sum_{i=1}^N \left(P_{RX,i} - \tilde{P}_{TX} + L_i \right)^2 \right). \quad (3)$$

B. Data Fusion and Feature Extraction

The augmented data is then utilized for setting up a Lightweight ICT-centric Mobility Simulation (LIMoSim) [24]

scenario. Although LIMoSim is actually a simulation framework for ground-based and aerial vehicular mobility, we utilize this unconventional method because of its rich environmental data aggregation capabilities that allow us to fuse the different data sources into a single methodological setup for further processing. For each receiver position \mathbf{p}_{RX} , different types of features are computed:

Receiver environment images: As one of its unique features, LIMoSim provides a dedicated Encapsulated Postscript (EPS) rendering engine capable of exporting vector screenshots of defined regions within the simulation scenario. DRaGon utilizes this approach for incorporating the raw top and side view images (examples are shown in Fig. 2) of the receiver environment into the machine learning process. Each top view image covers an area of $300 \text{ m} \times 300 \text{ m}$ with centered receiver position \mathbf{p}_{RX} . A normalization of the image rotation is performed such that the right axis always points towards the base station. This parameterization is chosen with respect to previous work [21], which also provides formal description of the export procedure. For generating the side view images, a simple direct path ray tracing is performed for determining the intersections points with terrain and buildings. Within these images, the receiver is vertically centered at the left edge and different colors are chosen for buildings (*black*) and terrain (*gray*). Finally, the vector images are converted into 64×64 -rasterized representations \mathbf{I}_{top} and \mathbf{I}_{side} to allow their utilization as Neural Network (NN) input features.

Numerical features: In addition to the images, several numerical features are extracted from the LIMoSim scenario. The aggregated feature vector \mathbf{x} aggregates information from different logical domains:

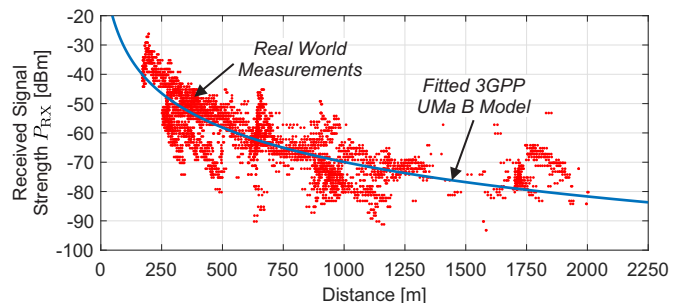


Fig. 3. Example for the estimation of the cell-specific EIRP \tilde{P}_{TX} by fitting available real world measurements to an UMa B channel model.

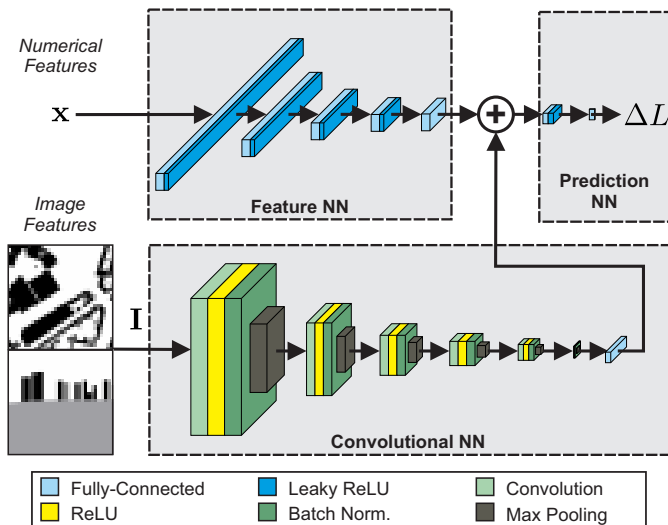


Fig. 4. Schematic illustration of the final deep neural network architecture.

- *Relative locations*: Absolute latitudinal and longitudinal distances Δ_{lon} and Δ_{lat} of receiver and transmitter
- *Direct path*: Distance d between receiver and transmitter, Number of building intersections N_{obs} , Indoor distance d_{obs} , Number of terrain intersections N_{ter} , Terrain distance d_{ter}
- *Communication system*: Bandwidth B , Carrier frequency f , Transmission power estimation \tilde{P}_{TX}

C. Deep Learning-Enabled RSRP Prediction

As illustrated in Fig. 4, the derived features are fed into a deep neural network that consists of three sub-NNs, which handle dedicated processing tasks. The *feature NN* is utilized for processing the numerical features \mathbf{x} using a sequence of processing blocks that perform linear transformations of the input data using the learned connection weights, followed by element-wise Rectified Linear Unit (ReLU) activation and batch normalization. In addition, the vertically concatenated images $\mathbf{I} = [\mathbf{I}_{top}^T, \mathbf{I}_{side}^T]^T$ are handled by the *convolutional NN*. Each processing block of the pipeline consists of a convolution layer with zero padding followed by ReLU activation, batch normalization and 2×2 max pooling. The final flattening of the two-dimensional input to the one-dimensional output is performed by the final linear layer. The derivation of the target variable ΔL is then performed using the *prediction NN*. Finally, the RSRP is predicted using Eq. 2.

IV. METHODOLOGY

Evaluation scenarios: For the performance evaluation, we consider real world measurements from different data sources:

- Vehicular measurements from the German city *Dortmund* [8] in campus, urban, suburban, and highway environments with three MNOs (68314 data samples)
- Vehicular measurements from the German city *Wuppertal* [4] in the networks of three MNOs (41113 data samples)
- Vehicular measurements from the Danish city *Kopenhagen* [6] in a campus environment (57586 data samples)
- Unmanned Aerial Vehicle (UAV) measurements from the Danish city *Aarhus* [25] (268534 data samples)

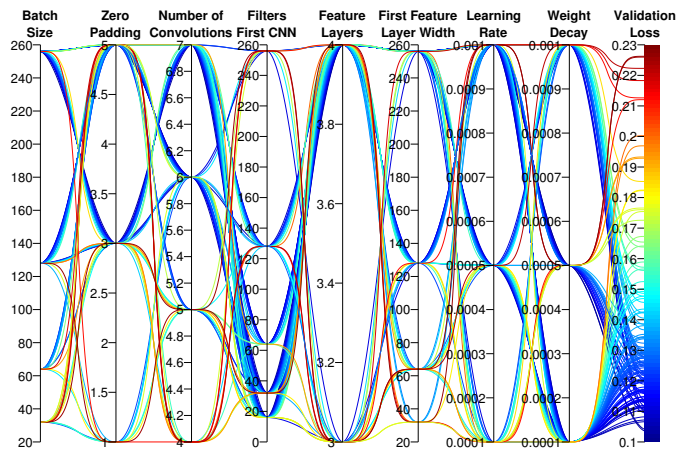


Fig. 5. Determination of the deep learning hyperparameter configuration using Bayesian optimization.

Validation methods: In addition to the real world measurements, multiple validation methods are used as references:

- *Conventional channel* models such as Friis, Nakagami ($m = 2$), and Two-Ray Ground
- *Empirical channel* modeling with 3GPP UMa B [15] and WINNER II C2 NLOS
- *Environment-aware* models with Obstacle shadowing [26] and Altair WinProp ray tracing

The machine learning evaluations are performed with PyTorch and accelerated with an Nvidia Tesla K40M with 2880 Compute Unified Device Architecture (CUDA) cores. For the training, the overall data set \mathcal{D} is split into 80% training data \mathcal{D}_{train} , 10% test data \mathcal{D}_{test} , and 10% validation data \mathcal{D}_{val} . For increasing the significance and repeatability of our results, our methodological setup is provided in an Open Source manner¹. A summary of the resulting parameterization of is shown in Tab. I.

TABLE I
FINAL CONFIGURATION OF THE DRAGON HYPERPARAMETERS

Hyperparameter	Value
Stride	1
Dilation	1
Batch Size	128
Zero Padding	3
CNN Filters	[32, 16, 16, 16, 10, 1]
Max Pooling	[2, 2, 2, 2, 2, 2]
Kernels	[5, 3, 3, 3, 3, 2]
Feature NN	[256, 128, 64, 32]
Prediction NN	[16]
Learning Rate	0.001
Weight Decay	0.0005
Optimizer	Adam

V. RESULTS

In the following, a sequential approach for analyzing the performance of the novel method is presented. After the initial hyperparameter optimization phase, the performance of DRaGon is evaluated on the *Dortmund* data set and compared to the reference methods. Finally, the generalizability of the proposed approach is discussed by taking the other evaluation scenarios into account.

¹The source code of the proposed DRaGon method is available at <https://github.com/melgeis/DRaGon>

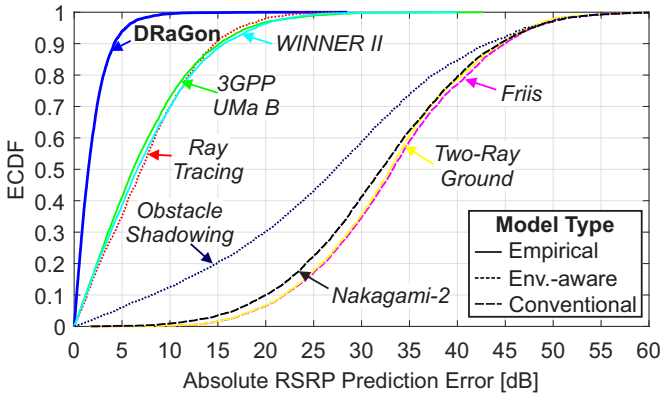


Fig. 6. Comparison of the absolute RSRP prediction errors of different methods using the *Dortmund* data set.

Hyperparameter optimization: In order to find the most suitable parameterization for DRaGon, Bayesian optimization is applied using the *wandb* toolkit. Hereby, a probabilistic model of the objective function is constructed and the relationship of the different hyperparameters is learned through sequential integration of the achieved knowledge of previous training runs. The parallel coordinate plot in Fig. 5 allows to investigate the trends of the 213 investigated hyperparameter combinations. In addition, it also illustrates the sensitivity of the target variable with respect to the hyperparameter values. It can be observed that the most important influence factors are the number of convolutions as well as the depth and width of the feature NN.

Performance comparison and validation: The behavior of the absolute RSRP prediction error of the considered methods is shown in Fig. 6 for the *Dortmund* data set. It can be seen that major differences rather occur between different model categories than between the individual models themselves. While the highest prediction accuracy (2.7 dB RMSE) is achieved by the proposed DRaGon method, the ray tracing approach shows a significantly higher prediction error (9.2 dB RMSE), similar to the empirical methods that achieve 9.3 dB to 9.6 dB RMSE. In compliance with [6], this observation shows that the performance of the ray tracing approach is significantly limited by the comparably coarse-grained OSM data. Moreover, in our evaluations, ray tracing achieves an approximately four times lower temporal efficiency than DRaGon. It is remarked that the analytical models also make use of the transmission power estimation for \tilde{P}_{TX} (see Sec. III-A) and thus might be optimistic towards the 3GPP UMa model. The conventional channel models show a significantly lower prediction accuracy as they do not account for the obstacles within the environment. Each of the considered methods achieves at least 33 dB RMSE, which highly limits their practical applicability. For DRaGon, it is further remarked that no significant differences of the prediction accuracy were identified for different MNOs and carrier frequency bands.

Generalizability: In order to analyze the generalizability of the proposed method over different scenarios, multiple data aggregation approaches are compared. While the *scenario-wise* approach performs an individual split evaluation (see Sec. IV) for each scenario, the *global* model is trained using 80 % of

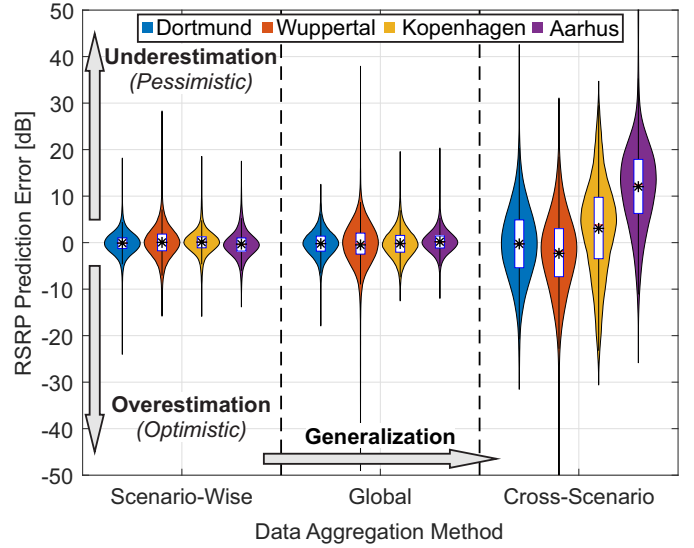


Fig. 7. Comparison of the scenario-specific prediction accuracy of DRaGon using different data aggregation methods. In contrast to the other scenarios that utilize ground-based vehicular measurement data, the *Aarhus* data contains UAV measurements at different altitudes.

the aggregated data. Finally, a *cross-scenario* evaluation is performed. For each of the i scenario subsets, \mathcal{D}_i is selected as the test set $\mathcal{D}_{\text{test}}$. The remaining data sets jointly form the training set $\mathcal{D}_{\text{train}}$. Fig. 7 shows the RSRP prediction error for the different data aggregation methods and evaluation scenarios. The consequences of prediction errors highly depend on the targeted use case: While RSRP underestimations can lead to violations of regulation thresholds within network planning, overestimations of the network quality can lead to inefficient resource usage in anticipatory mobile networking. Although it is well-known that the training data of machine learning methods should show a high grade of versatility for achieving good generalization [27], sometimes a better scenario-specific behavior can be achieved by increasing the grade of locality of the models. DRaGon shows no significant differences between those two approaches as the scenario-wise and the global data aggregation methods achieve a very similar behavior with zero mean for all evaluation scenarios. For the generalization, the most challenging method is the cross-scenario evaluation as it reveals the structural differences between the training data sets. As both German scenarios contain measurements from similar environment types (urban, suburban, rural, highway), a comparably high cross-scenario prediction accuracy is achieved for *Dortmund* and *Wuppertal*. In contrast to that, the *Kopenhagen* data does only contain campus measurements with moderate LOS dynamics and low vehicle speeds. As the cross-scenario evaluation excludes this data subset from the model training, the properties of the German radio measurements are overemphasized, leading to an underestimation of the less challenging *Kopenhagen* environment. The *Aarhus* data set exclusively contains UAV measurements at receiver heights up to 100 m. As the elevation angle increases with higher flight altitudes, the LOS probability is also increased. However, DRaGon is not able to learn this aspect if only ground-based vehicular measurements are utilized for the training. As a consequence, DRaGon behaves pessimistically and underestimates the signal

strength.

It is remarked that the *Dortmund* and *Wuppertal* data sets of [8] have been acquired using the native Android Application Programming Interface (API) with a sampling interval of 1 s. As a consequence, there exists a measurement-related inaccuracy in determining the receiver location even for perfect Global Navigation Satellite System (GNSS) fixes. For the highway track with maximum driven velocity of 150 km/h, this error can be up to 42 m. Since the DRaGon approach is sensitive to the quality of the geospatial information, future work should utilize more precise GNSS sensors within the data acquisition phase.

VI. CONCLUSION

In this paper, we presented the novel DRaGon method for RSRP prediction through extracting latent radio propagation information from geographical data. As demonstrated in a comprehensive performance evaluation campaign, the combination of expert knowledge and machine learning allows to achieve more accurate prediction results than existing methods such as analytical channel modeling and ray tracing. It is well-known in data science literature [27] that often, machine learning models benefit more from additional training data than from fine-tuning of the model hyperparameters. Therefore, we aim to further increase the versatility and the quality of our training data. In future work, we plan to utilize and further improve DRaGon in the context of machine learning-enabled network planning [28]. In addition we will consider more lightweight machine learning models [29] for achieving a better computational efficiency during training and inference.

ACKNOWLEDGMENT

This work has been supported by the German Research Foundation (DFG) within the Collaborative Research Center SFB 876 "Providing Information by Resource-Constrained Analysis", projects A4 and B4, as well as by the Ministry of Economic Affairs, Innovation, Digitalisation and Energy of the State of North Rhine-Westphalia (MWIDE NRW) along with the *Competence Center 5G.NRW* under grant number 005-01903-0047 and the project *Plan&Play* under the funding reference 005-2008-0047.

REFERENCES

- [1] A. Taufique, M. Jaber, A. Imran, Z. Dawy, and E. Yacoub, "Planning wireless cellular networks of future: Outlook, challenges and opportunities," *IEEE Access*, vol. 5, pp. 4821–4845, 2017.
- [2] E. R. Cavalcanti, J. A. R. de Souza, M. A. Spohn, R. C. d. M. Gomes, and A. F. B. F. d. Costa, "VANETs' research over the past decade: Overview, credibility, and trends," *SIGCOMM Comput. Commun. Rev.*, vol. 48, no. 2, pp. 31–39, May 2018.
- [3] N. Bui, M. Cesana, S. A. Hosseini, Q. Liao, I. Malanchini, and J. Widmer, "A survey of anticipatory mobile networking: Context-based classification, prediction methodologies, and optimization techniques," *IEEE Communications Surveys & Tutorials*, 2017.
- [4] B. Sliwa, R. Adam, and C. Wietfeld, "Client-based intelligence for resource efficient vehicular big data transfer in future 6G networks," *IEEE Transactions on Vehicular Technology*, Feb 2021.
- [5] Z. Yun and M. F. Iskander, "Ray tracing for radio propagation modeling: Principles and applications," *IEEE Access*, vol. 3, pp. 1089–1100, 2015.
- [6] J. Thrane, D. Zibar, and H. L. Christiansen, "Model-aided deep learning method for path loss prediction in mobile communication systems at 2.6 GHz," *IEEE Access*, vol. 8, pp. 7925–7936, 2020.
- [7] S. Ali, W. Saad, N. Rajatheva, K. Chang, D. Steinbach, B. Sliwa, C. Wietfeld, K. Mei, H. Shiri, H.-J. Zepernick, T. M. C. Chu, I. Ahmad, J. Huusko, J. Suutala, S. Bhadauria, V. Bhatia, R. Mitra, S. Amuru, R. Abbas, B. Shao, M. Capobianco, G. Yu, M. Claes, T. Karvonen, M. Chen, M. Girnyk, and H. Malik, "6G white paper on machine learning in wireless communication networks," Apr 2020.
- [8] B. Sliwa and C. Wietfeld, "Data-driven network simulation for performance analysis of anticipatory vehicular communication systems," *IEEE Access*, Nov 2019.
- [9] C. Wang, J. Huang, H. Wang, X. Gao, X. You, and Y. Hao, "6g wireless channel measurements and models: Trends and challenges," *IEEE Vehicular Technology Magazine*, vol. 15, no. 4, pp. 22–32, 2020.
- [10] I. Goodfellow, Y. Bengio, and A. Courville, *Deep Learning*. MIT Press, 2016, <http://www.deeplearningbook.org>.
- [11] 5GAA, "White paper: Making 5G proactive and predictive for the automotive industry," 5G Automotive Association, Tech. Rep., Jan 2020.
- [12] T. Pögel and L. Wolf, "Optimization of vehicular applications and communication properties with connectivity maps," in *2015 IEEE 40th Local Computer Networks Conference Workshops (LCN Workshops)*, Oct 2015, pp. 870–877.
- [13] A. Kliks, L. Kulacz, P. Kryszkiewicz, H. Bogucka, M. Dryjanski, M. Isaksson, G. P. Koudouridis, and P. Tengkvist, "Beyond 5G: Big data processing for better spectrum utilization," *IEEE Vehicular Technology Magazine*, vol. 15, no. 3, pp. 40–50, 2020.
- [14] W. Viriyasitavat, M. Boban, H. Tsai, and A. Vasilakos, "Vehicular communications: Survey and challenges of channel and propagation models," *IEEE Vehicular Technology Magazine*, vol. 10, no. 2, pp. 55–66, 2015.
- [15] "3GPP TR 38.901 - Study on channel model for frequencies from 0.5 to 100 GHz, V 16.1.0," 3rd Generation Partnership Project (3GPP), Tech. Rep. 38.901, Dec 2019.
- [16] C. Sommer, D. Eckhoff, and F. Dressler, "IVC in cities: Signal attenuation by buildings and how parked cars can improve the situation," *IEEE Transactions on Mobile Computing*, vol. 13, no. 8, pp. 1733–1745, 2014.
- [17] J. Wang, C. Jiang, H. Zhang, Y. Ren, K. Chen, and L. Hanzo, "Thirty years of machine learning: The road to pareto-optimal wireless networks," *IEEE Communications Surveys Tutorials*, pp. 1–1, 2020.
- [18] R. Enami, D. Rajan, and J. Camp, "RAIK: Regional analysis with geodata and crowdsourcing to infer key performance indicators," in *2018 IEEE Wireless Communications and Networking Conference (WCNC)*, April 2018, pp. 1–6.
- [19] U. Masood, H. Farooq, and A. Imran, "A machine learning based 3D propagation model for intelligent future cellular networks," in *2019 IEEE Global Communications Conference (GLOBECOM)*, Dec 2019, pp. 1–6.
- [20] M. E. Morocho-Cayamcela, M. Maier, and W. Lim, "Breaking wireless propagation environmental uncertainty with deep learning," *IEEE Transactions on Wireless Communications*, vol. 19, no. 8, pp. 5075–5087, 2020.
- [21] J. Thrane, B. Sliwa, C. Wietfeld, and H. Christiansen, "Deep learning-based signal strength prediction using geographical images and expert knowledge," in *2020 IEEE Global Communications Conference (GLOBECOM)*, Taipei, Taiwan, Dec 2020.
- [22] "3GPP TS 38.215 - Physical layer measurements, V 16.4.0," 3rd Generation Partnership Project (3GPP), Tech. Rep., Dec 2020.
- [23] A. Bashfield and A. Keim, "Continent-wide DEM creation for the European Union," in *34th International Symposium on Remote Sensing of Environment*, Apr. 2011.
- [24] B. Sliwa, M. Patchou, and C. Wietfeld, "Lightweight simulation of hybrid aerial- and ground-based vehicular communication networks," in *2019 IEEE 90th Vehicular Technology Conference (VTC-Fall)*, Honolulu, Hawaii, USA, Sep 2019.
- [25] M. Lopez, T. B. Sorensen, P. Mogensen, J. Wigard, and I. Z. Kovacs, "Shadow fading spatial correlation analysis for aerial vehicles: Ray tracing vs. measurements," in *2019 IEEE 90th Vehicular Technology Conference (VTC2019-Fall)*, 2019, pp. 1–5.
- [26] C. Sommer, D. Eckhoff, R. German, and F. Dressler, "A computationally inexpensive empirical model of IEEE 802.11p radio shadowing in urban environments," in *2011 Eighth International Conference on Wireless On-Demand Network Systems and Services*, 2011, pp. 84–90.
- [27] P. Domingos, "A few useful things to know about machine learning," *Commun. ACM*, vol. 55, no. 10, p. 78–87, Oct. 2012.
- [28] C. Bektas, S. Böcker, B. Sliwa, and C. Wietfeld, "Rapid network planning of temporary private 5G networks with unsupervised machine learning," in *2021 IEEE 94th Vehicular Technology Conference (VTC-Fall)*, Virtual, Sep 2021.
- [29] B. Sliwa, N. Piatkowski, and C. Wietfeld, "LIMITS: Lightweight machine learning for IoT systems with resource limitations," in *2020 IEEE International Conference on Communications (ICC)*, Dublin, Ireland, Jun 2020, Best paper award.